Helical undulator based on partial redistribution of uniform magnetic field

N. Balal,[1] I. V. Bandurkin,[2,*] V. L. Bratman,[1,2] and A. E. Fedotov[2]

[1]*Ariel University, Ariel*

[2]*Institute of Applied Physics, Russian Academy of Sciences, 603950 Nizhny Novgorod, Russia*

(Received 9 August 2017; published 19 December 2017)

A new type of helical undulator based on redistribution of magnetic field of a solenoid by ferromagnetic helix has been proposed and studied both in theory and experiment. Such undulators are very simple and efficient for promising sources of coherent spontaneous THz undulator radiation from dense electron bunches formed in laser-driven photo-injectors.

DOI: 10.1103/PhysRevAccelBeams.20.122401

I. INTRODUCTION

Advanced laser-driven photo-injectors make possible formation of very dense picosecond and sub-picosecond electron bunches with charge of the order of 1 nC and moderate energy of 3–6 MeV [1–5]. Such bunches can be attractive for production of power THz electromagnetic pulses [6–13], if very strong mutual Coulomb longitudinal repulsion of bunch particles is prevented or mitigated. One of the recently proposed efficient methods for stabilization of the electron bunches length and for corresponding increase of their spontaneous Doppler-up-shifted terahertz undulator radiation energy [12,13] is based on development of the so-called negative-mass instability (NMI) [14–17] in the bunches moving in undulators. Implementation of the method requires the undulator field to be combined with a strong uniform axial guiding magnetic field [12,13]. Here, the "strong" means that the value of the uniform guiding magnetic field should be higher than the resonant value corresponding to the coincidence of undulator and cyclotron frequencies of the electrons. In this paper, we demonstrate that in such a system, the undulator field can be easily created by redistributing the strong uniform field by a periodic ferromagnetic helix. A similar method was proposed and demonstrated many years ago in planar undulator systems with periodic planar insertions [18–20]. Also, helically distributed planar elements were used for creating a relatively low helical transverse magnetic field [21]. We suggest using a more convenient helical undulator based on a fully-symmetrical helical insertion [22]. It is fairly obvious that magnetization of a ferromagnetic helix in the guiding field provides a helical component of the magnetic field, and we will show that a sufficient for realization of the NMI-based terahertz source amplitude of this component can be readily obtained.

II. ANALYTICAL ESTIMATING

According to [12,13], development of NMI inside a dense electron bunch can lead to effective mutual attraction of particles. As a result, a dense core with a fairly stable longitudinal size smaller than the radiation wavelength can appear. Such longitudinal bunching occurs in a combined helical, $\vec{B}_u$, and over-resonance uniform guiding, $B_0\vec{z}_0$, magnetic fields when the electron cyclotron frequency, $\omega_c = eB_0/m\gamma$, is larger than its undulator bounce-frequency, $\omega_u = 2\pi v_\parallel/d$. Here, e, m, γ and $v_\parallel$ are the electron charge, mass, Lorentz-factor, and longitudinal velocity, and d is the undulator period. In this over-resonance region of parameters, the increase of the energy, $mc^2\gamma$, of a front electron under the action of Coulomb field of the rest of the bunch causes approaching of the electron to the resonance, $\omega_c \approx \omega_u$. If the electrons move along their quasi-stationary helical trajectories, it is accompanied with increase of the transverse electron velocity, $v_\perp = cK/\gamma\Delta$, where $K = eB_u d/2\pi mc$ and $\Delta = 1 - \omega_c/\omega_u$ are the undulator parameter and the resonance mismatch. In certain conditions, the transverse velocity grows so quickly that the derivative $\partial v_\parallel/\partial\gamma$ is negative, and the longitudinal components of the front bunch particles velocities decrease. Simultaneously, particles from the rear part of the bunch lose their energy and move away from the resonance, which is accompanied with the decrease of transverse and increase of longitudinal components of velocities. Thus, similarly to the classic cyclotron negative-mass instability in cyclic accelerators [23,24] and gyrodevices [25–27], the change of the electrons energy in the repulsing Coulomb field leads to an effective longitudinal attraction and bunching of nonisochronously oscillating particles.

For typical parameters of a THz source, considered in [12,13] (particle energy of 5–6 MeV, bunch charge of up to 1 nC, and radiation frequency of 1–2 THz), the value of undulator field, B_u, should be of the order of 0.1–0.2 T, that is tens of times smaller than the guiding field, B_0.

*iluy@appl.sci-nnov.ru

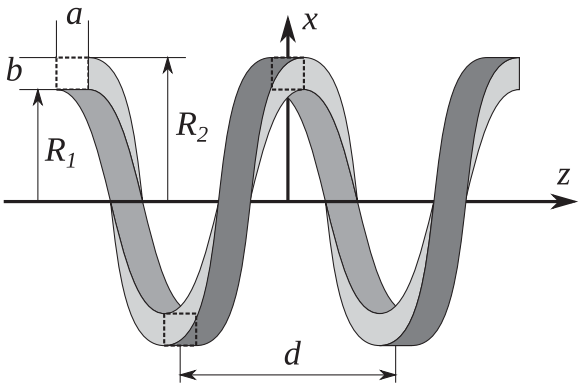

FIG. 1. Ferromagnetic helical insertion into solenoid (two periods are shown).

Correspondingly, a relatively thin steel helix is supposed to be sufficient for providing the required value of undulator field.

Let us find the field of a helical insertion placed into an infinite solenoid with a uniform field. Consider magnetization $\vec{J}$ of an infinite ferromagnetic helix with period (step) d, inner and outer radii R_1 and R_2, respectively, thickness $b = R_2 - R_1$, and axial size a (Fig. 1). In the case of a very strong guiding field, the magnetization of the helix is saturated, $\vec{J} = \vec{J}_\infty$, so that its direction practically coincides with direction of the field, $\vec{z}_0$, and its value does not depend on B_0.

Let us consider an elementary thin helix, for which $R_1 \approx R_2 \approx R$, $b \ll R$, and introduce its surface magnetization. Taking into account that the helix bulk is periodic in axial direction and invariant to the transformations keeping $\varphi + 2\pi z/d = \text{const}$, we use the Fourier expansion and represent the magnetization in the form

$$\vec{J}(r,\varphi,z) = bJ_\infty \delta(r-R)\vec{z}_0 \sum_{n=-\infty}^{\infty} f_n e^{in(hz+\varphi)}, \quad (1)$$

where $h = 2\pi/d$ and $f_n = (1/\pi n)\sin(nha/2)$. The nth harmonic of the magnetization, $\vec{J}_n$, presents a continuous polarized cylindrical surface with radius R; $\mathrm{div}\vec{J}_n$ can be interpreted as equivalent continuously distributed surface magnetic charge. The corresponding harmonic of the static magnetic potential satisfies the Poisson equation

$$\Delta\psi_n = \mathrm{div}\vec{J}_n. \quad (2)$$

Boundary conditions at the cylindrical surface $r = R$ correspond to continuity of the potential and jump of the radial component of magnetic field strength $\vec{H}_n = -\nabla\psi_n$:

$$[\psi_n]_{r=R} = 0, \qquad [H_r]_{r=R} = -inhbRJ_\infty f_n e^{in(hz+\varphi)}. \quad (3)$$

The solution of Eqs. (2), (3) is

$$\psi_n = -ing_n e^{in(hz+\varphi)} \begin{cases} \mathrm{K}_p(phR)\mathrm{I}_p(phr), & r \le R \\ \mathrm{I}_p(phR)\mathrm{K}_p(phr), & r \ge R \end{cases}, \quad (4)$$

where I_p, K_p are modified Bessel and McDonald functions of the order of $p = |n|$ and $g_n = hbRJ_\infty f_n$.

It is easy to show that only harmonics $n = \pm 1$ in Eq. (4) contribute to the transverse undulator field at the axis of the system. The corresponding field is

$$\vec{B}_u(r=0) = \Re[(\vec{x}_0 + i\vec{y}_0)B_u e^{i(hz-\pi/2)}], \quad (5)$$

where

$$B_u = \frac{1}{\pi} h^2 Rb \sin(ha/2)\mathrm{K}_1(hR)\mu_0 J_\infty. \quad (6)$$

Maximum of the transverse field is achieved when the longitudinal size of the helix is equal to half of its period, $a = d/2$. Integration of expression (4) over the radius gives solution for the helix of finite thickness.

III. NUMERICAL SIMULATIONS

The applicability of the solution (5)–(6) was verified by direct solving of magnetostatic equations using *CST Studio*. This code allows one to take into account a finite thickness, arbitrary transverse and longitudinal profiles of the helix as well as nonlinear dependence of magnetic permeability of steel on applied field. Numerical simulations demonstrate a high accuracy of the solution (5)–(6) for long enough helices. For instance, the estimation (6) yields for the case of an iron helix having the parameters of $d = 2.5$ cm, $a = 1.2$ cm, $R_1 = 0.3$ cm and $b = 0.2$ cm the value of the transverse magnetic field of 0.24 T, which admits quite well with 0.21 T given by the *CST Studio* simulations for these parameters and axial magnetic field of $8\text{T} \gg \mu_0 J_\infty \approx 2.15$ T (Fig. 2).

Also, formula (6) can be well applied for thin helices with round cross sections if one takes parameters a and b equal to each other, so that ab corresponded to the square of the wire cross section, and R equal to the mean radius of the helix bulk (Fig. 3).

IV. EXPERIMENTAL MEASUREMENTS

The described method of creation of helical undulator field has been also studied experimentally for a helix of square cross section (Fig. 4). In the experiment, using a probe in the form of a small coil, the transverse field was measured on the axis of the helix placed into pulsed fields with maximum values of 4–5 T. The probe coil contained ~200 turns and had a length of 5 mm and an average diameter of 5 mm. To compensate for the inevitable deviation of the coil axis from the radial direction, leading to a contribution from the strong longitudinal field, the probe was rotated around the main solenoid (z) axis, and a

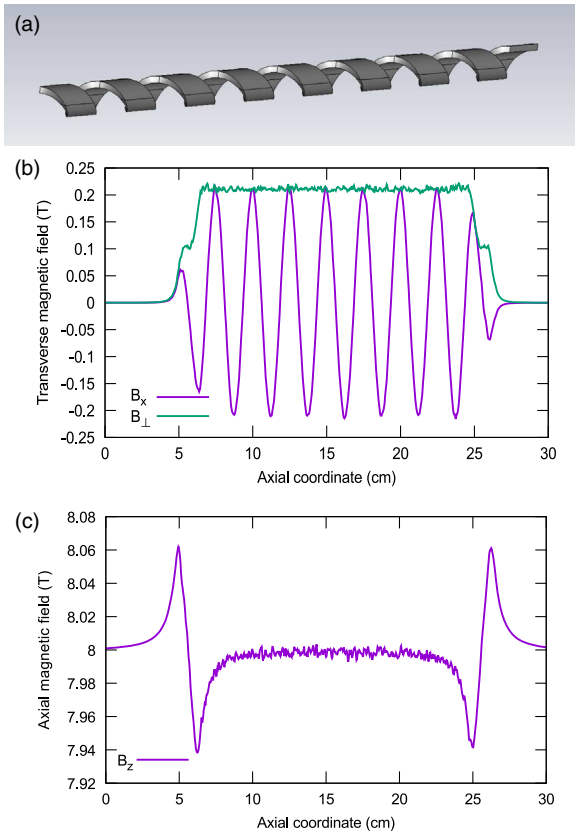

FIG. 2. Results of simulations within the *CST Studio* for the case of steel helix with rectangular cross section having the parameters of $d = 2.5$ cm, $a = 1.2$ cm, $R_1 = 0.3$ cm and $b = 0.2$ cm. The helix geometry (a) and the amplitudes of the transverse (b) and axial (c) magnetic fields.

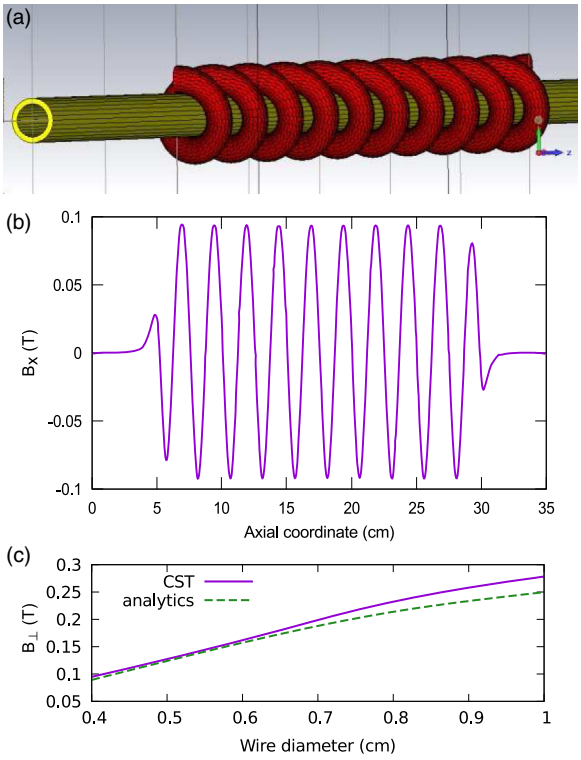

FIG. 3. Results of simulations within the *CST Studio* for the case of iron helix with round cross section, period of 2.5 cm, and inner radius of 5 mm. The helix geometry (a) and the amplitude of the transverse magnetic field as function of axial coordinate [(b), wire diameter is 0.4 cm] and of helix wire diameter [(c), maximum field amplitude]. The predictions of formula (6) for the equivalent square cross section are also shown (c).

constant component was subtracted from the measured value.

In the first experiment, we used a steel helix with the period of 2.5 cm, inner radius of 0.6 cm and square cross section having thickness of 0.4 cm [Fig. 4(a)]. The steel type was equivalent to ASTM-SAE 1045 having the carbon content less than 0.5%, which means that the saturation magnetic field was about 2 T [28]. The helix was manufactured from steel cylinder first by milling the cylinder surface and then by cutting away the inner part by electrical discharge machining. Being mounted in the pulsed solenoid with an axial magnetic field of about 4.5 T, it created the transverse helical field of the order of 0.1 T (Fig. 5). The main source of measurements error was connected with displacements of the probe coil from the solenoid axis, which were caused partially by misalignment of the probe support during the rotation of the probe, and partially by mechanical shakes caused by pulsed magnetic field of large amplitude. The difference in field values measured at different axial probe positions can be explained by the axial inhomogeneity of the solenoid field, which had the axial scale of about 10 cm. It should be noted, that in real application, such a helix is supposed to be placed inside a DC or long-pulse solenoid, whereas in the described experiment, the solenoid pulse had an almost sinusoidal form, $B_0 \sim \sin(\pi t/T)$, with a length of "half-period" $T \approx 3$ ms. In principle, in the pulsed case, a second source of transverse magnetic field appears, which is the induction current along the helix. Nevertheless, simple estimations show that for these particular pulse duration, helix geometry and material conductance, the correspondent magnetic field is almost two orders of magnitude lower than the one induced by magnetization.

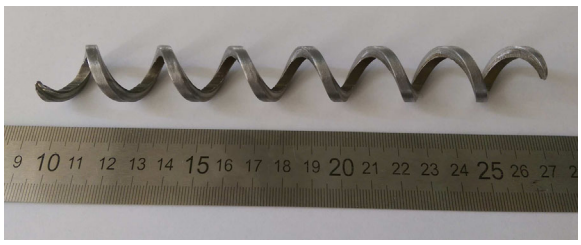

FIG. 4. Steel helix with square cross section used for experimental measurements of induced transverse magnetic field.

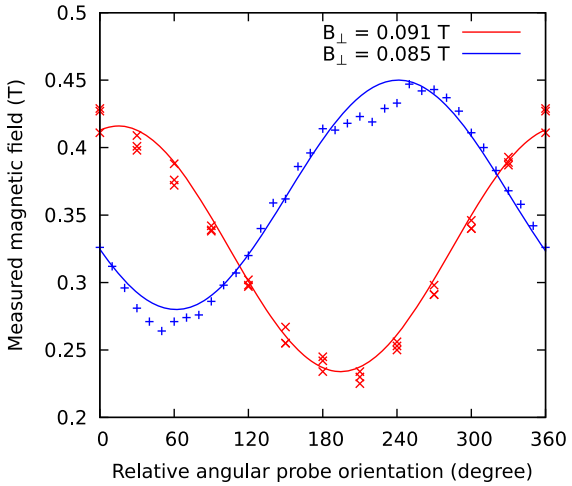

FIG. 5. Results of experimental measuring of a transverse magnetic field at the axis of the steel helix of a square cross section. The different curves correspond to different axial positions of the probe. The transverse component of the field is determined as an amplitude of the sinlike dependency of the probe signal on its angular position.

It is very important, that the simple formulas (5)–(6) give for the experimental parameters the very same value of transverse magnetic field, $B_u \approx 0.09$ T, and so do the *CST* numerical simulations. This proves the correctness of theoretical calculations and assures that the undulator field of 0.2 T, which was predicted by calculations of Sec. III and corresponds to desirable undulator parameter, $K \approx 0.5$, indeed can be achieved experimentally.

V. CONCLUSION

The proposed method of creating a helical undulator field by redistributing the uniform field at a steel helix seems very simple and efficient. It can be naturally applied to THz sources of coherent spontaneous undulator radiation using the NMI stabilization of longitudinal sizes of short picosecond and subpicosecond electron bunches [12,13]. According to simulations, development of NMI in a combined strong uniform and helical undulator fields can provide maintenance of nearly constant sizes of short and long-living bunch cores at a fairly large undulator length. It makes possible the implementation of powerful and narrowband radiation sources with initial electron energy of about 5–6 MeV and charge of the order of 1 nC with the frequency of 1–2 THz and efficiency of about of 20%.

ACKNOWLEDGMENTS

The authors are grateful to A. V. Savilov for useful discussions. The work is supported by Russian Foundation for Basic Research, Project No. 16-02-00794, and by Israeli Ministry of Science, Technology and Space.

[1] J. Power, Overview of photoinjectors, AIP Conf. Proc. **1299**, 20 (2010).
[2] A. Bartnik, C. Gulliford, I. Bazarov, L. Cultera, and B. Dunham, Operational experience with nanocoulomb bunch charges in the cornell photoinjector, Phys. Rev. ST Accel. Beams **18**, 083401 (2015).
[3] F. Stephan, C. H. Boulware, M. Krasilnikov, J. Bähr, G. Asova, A. Donat, U. Gensch, H. J. Grabosch, M. Hänel, L. Hakobyan *et al.*, Detailed characterization of electron sources yielding first demonstration of european x-ray free-electron laser beam quality, Phys. Rev. ST Accel. Beams **13**, 020704 (2010).
[4] J. B. Rosenzweig, A. Valloni, D. Alesini, G. Andonian, N. Bernard, L. Faillace, L. Ficcadenti, A. Fukusawa, B. Hidding, M. Migliorati *et al.*, Design and applications of an x-band hybrid photoinjector, Nucl. Instrum. Methods Phys. Res., Sect. A **657**, 107 (2011).
[5] K. J. Pérez Quintero, S. Antipov, A. V. Sumant, C. Jing, and S. V. Baryshev, High quantum efficiency ultrananocrystalline diamond photocathode for photoinjector applications, Appl. Phys. Lett. **105**, 123103 (2014).
[6] A. Doria, R. Bartolini, J. Feinstein, G. P. Gallerano, and R. H. Pantell, Coherent emission and gain from a bunched electron beam, IEEE J. Quantum Electron. **29**, 1428 (1993).
[7] A. Gover, F. V. Hartemann, G. P. Le Sage, N. C. Luhmann, Jr, R. S. Zhang, and C. Pellegrini, Time and Frequency Domain Analysis of Superradiant Coherent Synchrotron Radiation in a Waveguide Free-Electron Laser, Phys. Rev. Lett. **72**, 1192 (1994).
[8] Y. Lurie and Y. Pinhasi, Enhanced super-radiance from energy-modulated short electron bunch free-electron lasers, Phys. Rev. ST Accel. Beams **10**, 080703 (2007).
[9] Y. Lurie, A. Friedman, and Y. Pinhasi, Single pass, THz spectral range free-electron laser driven by a photocathode hybrid rf linear accelerator, Phys. Rev. ST Accel. Beams **18**, 070701 (2015).
[10] V. L. Bratman, D. A. Jaroszynski, S. V. Samsonov, and A. V. Savilov, Generation of ultra-short quasi-unipolar electromagnetic pulses from quasi-planar electron bunches, Nucl. Instrum. Methods Phys. Res., Sect. A **475**, 436 (2001).
[11] K. Lee, J. Mun, S. H. Park, K.-H. Jang, Y. U. Jeong, and N. A. Vinokurov, Numerical investigation of the radiation characteristics of a variable-period helical undulator, Nucl. Instrum. Methods Phys. Res., Sect. A **776**, 27 (2015).
[12] N. Balal, I. V. Bandurkin, V. L. Bratman, E. Magory, and A. V. Savilov, Negative-mass mitigation of coulomb repulsion for terahertz undulator radiation of electron bunches, Appl. Phys. Lett. **107**, 163505 (2015).
[13] Y. Lurie, V. L. Bratman, and A. V. Savilov, Energy enhancement and spectrum narrowing in terahertz electron sources due to negative mass instability, Phys. Rev. Accel. Beams **19**, 050704 (2016).
[14] H. P. Freund and P. Sprangle, Unstable electrostatic beam modes in free-electron-laser systems, Phys. Rev. A **28**, 1835 (1983).
[15] A. K. Ganguly and H. P. Freund, Nonlinear analysis of free-electron-laser amplifiers in three dimensions, Phys. Rev. A **32**, 2275 (1985).

[16] N. S. Ginzburg and N. Y. Peskov, Non-linear theory of relativistic ubitrons with electron beams, formed in the adiabatically growing undulator field and homogeneous longitudinal magnetic field, Tech. Phys. **58**, 859 (1988).

[17] H. P. Freund and T. M. Antonsen, *Principles of Free Electron Lasers* (Chapman and Hall, London, 1996).

[18] A. Ho, R. Pantell, J. Feinstein, and B. Tice, A novel wiggler design for use in a high-efficiency free-electron laser, Nucl. Instrum. Methods Phys. Res., Sect. A **296**, 631 (1990).

[19] A. A. Varfolomeev, A. S. Khlebnikov, S. N. Ivanchenkov, N. S. Osmanov, and A. H. Hairetdinov, Strong magnetic field microundulator with permanent magnets inserted into a solenoid, Nucl. Instrum. Methods Phys. Res., Sect. A **331**, 745 (1993).

[20] V. L. Bratman, A. V. Savilov, V. A. Papadichev *et al.*, FEM with pulsed short-period undulator and low-energy electron beam, in *Proceedings of 20th International Free Electron Laser Conference*, edited by G. R. Neil and S. V. Benson (Williamsburg, Virginia, 1998), pp. II–15.

[21] N. Ohigashi, Y. Tsunawaki, M. Fujita, K. Imasaki, K. Mima, and S. Nakai, Construction of compact fem using solenoid-induced helical wiggler, Nucl. Instrum. Methods Phys. Res., Sect. A **507**, 250 (2003).

[22] N. Balal, V. L. Bratman, and E. Magori, Efficient electron sources of coherent spontaneous radiation with combined helical and uniform magnetic fields, in *Proceedings of 37th International FEL Conference* (Daejeon, Korea, 2015), p. MOP009, http://inspirehep.net/record/1426210/.

[23] C. E. Nielsen and A. M. Sessler, Longitudinal space charge effects in particle accelerators, Rev. Sci. Instrum. **30**, 80 (1959).

[24] A. A. Kolomensky and A. N. Lebedev, Stability of charged beams in storage systems, At. Energ. **7**, 549 (1959).

[25] V. L. Bratman, Instability of orbital movement in a layer of electrons, rotating in uniform magnetostatic field. 2, Tech. Phys. **46**, 2030 (1976).

[26] V. L. Bratman and A. V. Savilov, "Phase mixing" of bunches and decrease of negative-mass instability increments in cyclotron resonance masers, Phys. Plasmas **2**, 557 (1995).

[27] A. V. Savilov, Negative-mass instability in magnetron-injection guns, Phys. Plasmas **4**, 2276 (1997).

[28] C. W. Burrows, Correlation of the magnetic and mechanical properties of steel, Bulletin of the Bureau of Standards **13**, 173 (1916).